

pubs.acs.org/JACS Article

# Universal Concept for Bright, Organic, Solid-State Emitters—Doping of *Small-Molecule Ionic Isolation Lattices* with FRET Acceptors

Laura Kacenauskaite, Stine G. Stenspil, Andrew H. Olsson, Amar H. Flood,\* and Bo W. Laursen\*



Cite This: J. Am. Chem. Soc. 2022, 144, 19981-19989



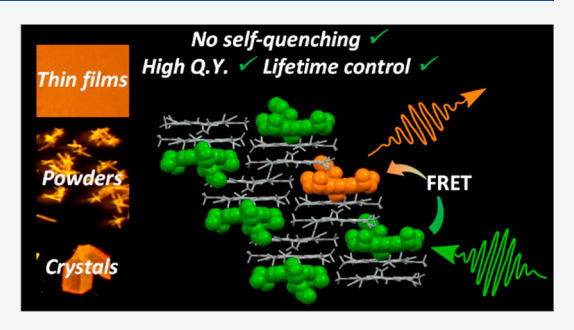
**ACCESS** 

III Metrics & More

Article Recommendations

Supporting Information

**ABSTRACT:** Brightly fluorescent solid-state materials are highly desirable for bioimaging, optoelectronic applications, and energy harvesting. However, the close contact between  $\pi$ -systems most often leads to quenching. Recently, we developed *small-molecule ionic isolation lattices* (SMILES) that efficiently isolate fluorophores while ensuring very high densities of the dyes. Nevertheless, efficient Förster resonance energy transfer (FRET) energy migration in such dense systems is inevitable. While attractive for energy harvesting applications, FRET also significantly compromises quantum yields of fluorescent solids by funneling the excitation energy to dark trap states. Here, we investigate the underlying property of FRET and exploit it to our favor by intentionally introducing fluorescent dopants into SMILES materials,



acting as FRET acceptors with favorable photophysical properties. This doping is shown to outcompete energy migration to dark trap states while also ruling out reabsorption effects in dense SMILES materials, resulting in universal fluorescent solid-state materials (thin films, powders, and crystals) with superior properties. These include emission quantum yields reaching as high as 50–65%, programmable fluorescence lifetimes with mono-exponential decay, and independent selection of absorption and emission maxima. The volume normalized brightness of these FRET-based SMILES now reach values up to 32,200 M<sup>-1</sup> cm<sup>-1</sup> nm<sup>-3</sup> and can deliver freely tunable spectroscopic properties for the fabrication of super-bright advanced optical materials. It is found that SMILES prohibit PET quenching between donor and acceptor dyes that is observed for non-SMILES mixtures of the same dyes. This allows a very broad selection of donor and acceptor dyes for use in FRET SMILES.

#### INTRODUCTION

Optoelectronic materials based on organic molecular solids are highly attractive for a range of emerging technologies <sup>1–4</sup> because organic synthesis provides vast opportunities for engineering specific properties into the molecular units. <sup>5–9</sup> However, key properties of the molecules are often lost, and new uncontrollable features emerge at the materials level. <sup>10–13</sup> Strong exciton coupling between transition dipoles of the molecular units in close proximity is responsible for these altered properties in the solid state, leading to unpredictable charge transport and emissive properties.

For OLEDs and organic photovoltaic materials, close orbital contact and molecular coupling are needed to ensure efficient charge transport, and large efforts are invested in trial and error structure optimization. <sup>12,14–17</sup> However, for emission-focused applications like solar concentrators, <sup>18,19</sup> laser gain media, <sup>20</sup> sensors and imaging labels <sup>21–25</sup> that do not require charge conduction, electronic decoupling is highly desirable. Efficient schemes for electronic decoupling of molecular dyes/chromophores in solids would enable their attractive photophysical properties, which have been optimized in the solution state over the last century of chemical research, to be transferred to dense solids for designing advanced optical materials.

Multiple methods to at least partially decouple fluorophores and reinstate solution-like properties in the solid state were developed over the years. The most straightforward approach is covalent modification with bulky side groups keeping the molecular  $\pi$ -systems apart. This method has been extensively used for both small molecules and polymers.<sup>7,25-27</sup> Some privileged chromophore motifs are, for various reasons, often emissive in the solid state.<sup>6,12</sup> Among these, much attention has been given to the so-called AIEgens<sup>28,29</sup> that typically are flexible chromophores with large internal relaxation and relatively weak optical transitions. Consequently, electronic coupling in solid AIE materials is limited. Most of the other methods to reinstate emission in the solid state rely on polymers, metal-organic frameworks, or nanoporous solids that act as matrixes to "dilute" fluorophores, ensuring adequate spacing and electronic decoupling. 24,30-35 Using these methods, quantum yields of the fluorophores embedded in

Received: August 11, 2022 Published: October 18, 2022





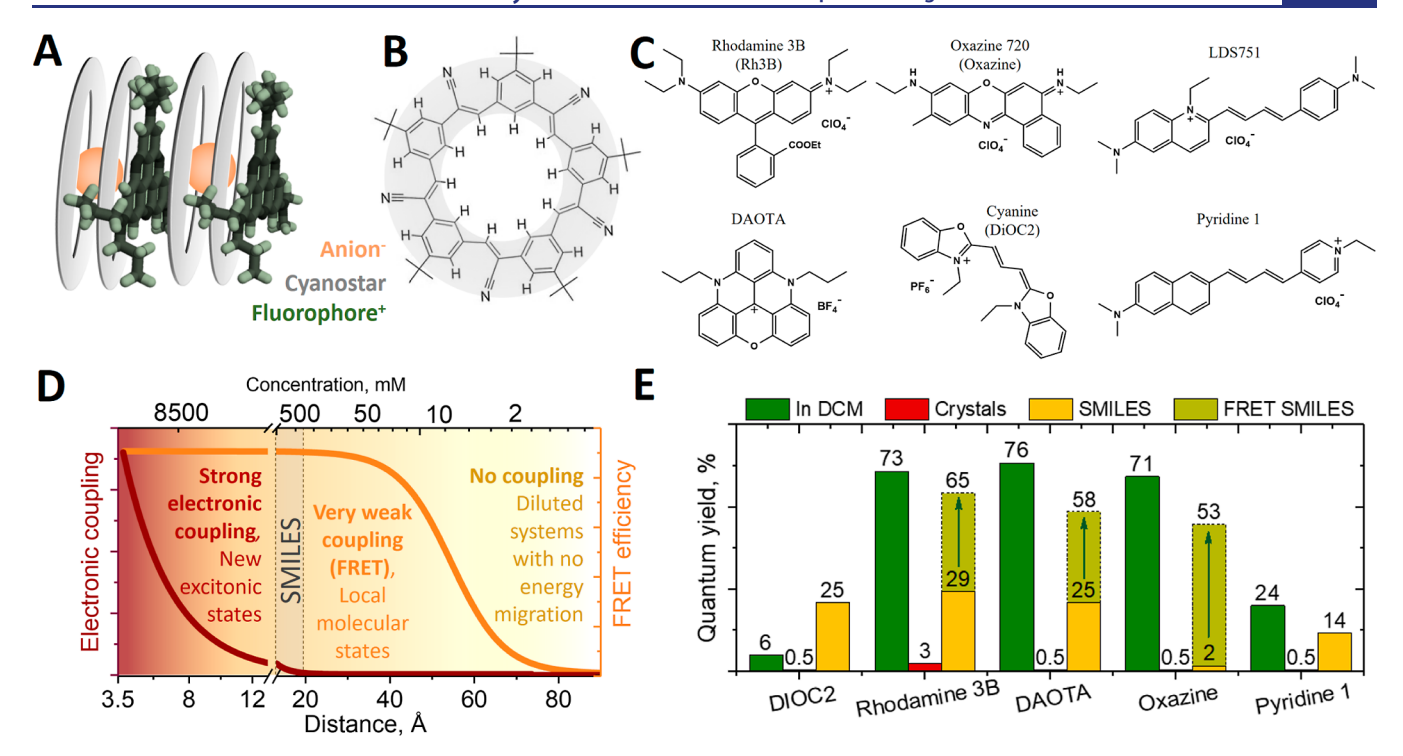


Figure 1. (A) Schematic representation of the molecular packing structure in SMILES materials. (B) Structure of the CS receptor. (C) Structure of the investigated cationic dyes. (D) Schematic of the electronic coupling strength (red line) and typical FRETefficiency (orange line) as a function of the distance between fluorophores and their corresponding concentration. (E) Fluorescence quantum yields of various fluorophores in DCM, solid-state (non-SMILES), as SMILES crystals, and their improvement upon FRET doping of SMILES reported in this work.

solid matrixes can reach as high as the ones observed in dilute solid solutions; however, it comes at the price of relatively low dye density and thus low volume-normalized brightness and/or with severe restrictions on the size/shape of the guest dye.

The ability to maximize emission brightness while keeping the density of the fluorophores as high as possible is a fundamental issue that calls for a general method to arrange fluorophores in a predictable manner. Strong Coulombic interactions between anions and cations act as a fundamental and strong organizing principle in salts, and replacement of small counteranions of cationic fluorophores with larger ones has emerged as a simple and efficient non-covalent approach to reduce dye—dye contact and lower electronic coupling. <sup>36–38</sup> Using this strategy, Reisch and Klymchenko have been able to increase the dye loading in polymers and reach high dye densities and brightness, though still at the price of reduced quantum yields. <sup>24,39–41</sup>

Anion-binding receptors offer a supramolecular approach to modify the size, shape, and properties of anions and thus packing of molecular salts. Taking this direction, we recently introduced a new and simple method to produce bright fluorescent solid-state materials from conventional organic dyes. Simply adding the anion-binding macrocycle cyanostar (CS) to cationic fluorophores induced predictable packing of the dyes into *small-molecule ionic isolation lattices* (SMILES, Figure 1A), where cationic fluorophores (green) are efficiently isolated from each other by the large disc-shaped anion complexes formed between anions (orange) and 2 equiv of CS (gray, Figure 1B), as sketched in Figure 1. As, 46 The SMILES concept has been demonstrated for a range of prevalent dye classes in both thin films and crystals, as well as in nanoparticles, 47,48 yielding both very high brightness and

high dye density in the solids (up to  $\sim$ 0.5 M, or one dye per 3.5 nm<sup>3</sup>).

We found significant improvement of photophysical properties upon the co-crystallization of various cationic dyes (Figure 1C) with CS, making SMILES crystals and nanoparticles among the brightest fluorescent molecular materials reported, with volume normalized brightness  $B_v = 7000 \text{ M}^{-1} \text{ cm}^{-1} \text{ nm}^{-3}$ (see Section S1 for details on volume-normalized brightness).<sup>45</sup> Yet, the perfectly predictable translation of all of the molecular chromophore's optical properties from solution to dense solids remains unfulfilled. Despite the reinstated spectral shapes and significantly higher quantum yields (up to 30%), SMILES materials are still partially quenched. This outcome is evidenced by fluorescence quantum yields that are at least a few times lower than those observed in dichloromethane (DCM) solutions (compare yellow bars to dark green bars in Figure 1E). We have in the past tentatively assigned these losses in potential performance to two effects: On the mesoscale, energy migration by Förster resonance energy transfer (FRET) between weakly coupled dyes in SMILES (Figure 1D) enables excitons to migrate to dark trap states. On the macroscale, the high optical density of solids causes reabsorption and lowering of the emission yield.

In this work, we first investigate and analyze the effects of FRET energy migration to quenching sites and of reabsorption in SMILES materials, then show how these unwanted, yet fundamental and general, effects in dense molecular materials can be bypassed by introduction of dopant dyes into SMILES to act as emission sites. Application of this knowledge leads us to fabricate a new type of molecular material: FRET SMILES, with fully predictable photophysical properties and highly increased fluorescence quantum yields that are now

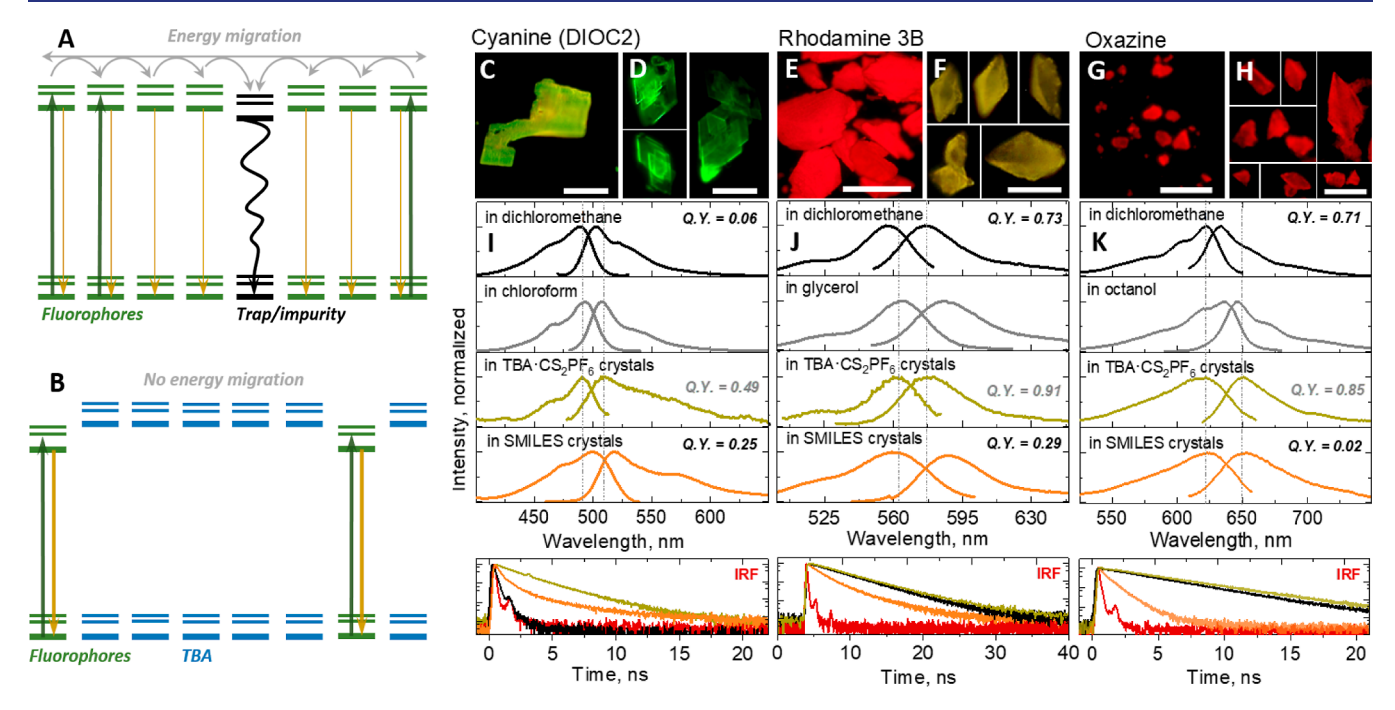


Figure 2. Energy migration pathways in densely packed fluorescent SMILES crystals. (A) State diagram representing energy migration pathways in the SMILES crystal. (B) State diagram representing diluted systems where low fractions of fluorophores (<1 mol %) are imbedded in TBA·CS<sub>2</sub>PF<sub>6</sub> crystals. (C,E,G) Fluorescence micrographs (ex. 475 nm, em.: 510 nm LP, scale bar— $100 \mu m$ ) of SMILES crystals containing specified dyes. (D,F,H) Fluorescence micrographs (ex. 475 nm, em.: 510 nm LP, scale bar— $20 \mu m$ ) of corresponding diluted SMILES crystals comprising 99.95% of TBA·CS<sub>2</sub>PF<sub>6</sub> and 0.05% of fluorophore·CS<sub>2</sub>PF<sub>6</sub>. (I–K) Excitation and emission spectra and fluorescence decays of specified fluorophores in different solvents and finely grinded solids (according to the color of traces).

comparable to those found in the dilute solutions (compare light green bars to dark green bars in Figure 1E).

## ■ RESULTS AND DISCUSSION

General Concept. To fully understand and further improve SMILES materials, we first set out to investigate the reason for fluorescence quantum yields being lower than those in solution. Based on a few key observations, we hypothesized that the reduced quantum yields originate from two effects: (1) reabsorption of emitted light due to the high optical density of crystals and (2) energy migration to dark trap states. Reabsorption (inner filter effects) in molecular crystals is a known issue<sup>51,52</sup> and is also clearly manifested for SMILES materials. We see larger crystals emitting more red-shifted fluorescence and spectra approaching the solution spectra only when they are either collected selectively from the surface using confocal microscopy (Figure S2) or when crystals were ground to smaller sizes (Figures S3A-G and S4).45 As expected, this effect is clearly correlated with the optical density of the solids (Figure S3H-J), which mainly relies on material dimensions and molar absorption coefficients since the packing density in SMILES is quite similar for all the dyes  $(\sim 3.5 \text{ nm}^3 \text{ per fluorophore}).^{45}$ 

Energy migration is expected to be quite efficient in SMILES (and all other materials with such high densities of strongabsorbing dyes). Therein, the distance between dyes ( $\approx$ 15 Å) is considerably shorter than the Förster distance for homotransfer ( $R_0 \approx 50$  Å) of dyes with strong absorption and a small Stokes shift (Figure 1D and Table S1). Thus, even with strong electronic coupling prohibited, SMILES have the potential to be considerably affected by impurities, defects in the crystal, or other energetically lower-lying traps states, Figure 2A. <sup>12,53</sup> By acting as quenchers for many dye units in their vicinity, such

traps will affect the observed quantum yields and fluorescence lifetimes. The most obvious manifestation of this effect is the non-mono-exponential fluorescence decays observed for both crystals and nanoparticles, resulting from the inhomogeneous spatial distribution of traps. 45,47 Increasing the distance between dyes far beyond the Förster distance should prohibit this mode of quenching, as known from highly diluted dyes in polymer particles, MOFs, and so forth. 47,54 By diluting the fluorescent dyes into crystals composed primarily of inert, transparent tetrabutylammonium cations (TBA) and CShexafluorophosphate anion complexes (CS<sub>2</sub>PF<sub>6</sub><sup>-</sup>), the excitons become locked on a single dye site (Figure 2B). By comparing these diluted systems to dense SMILES, we can observe the impact of reabsorption and trap states. These dilute SMILES materials also retain the local environment of dense SMILES materials. Therefore, this local similarity allows us to verify that the CS-anion complexes, do not have a negative impact on the photophysical properties of dyes.

Probing the Intrinsic Photophysical Properties of Dyes in SMILES. By decreasing the loading of fluorescent dyes in the TBA·CS<sub>2</sub>PF<sub>6</sub> crystals to less than 1% (dye-to-TBA mol %), emission becomes less red-shifted in contrast to conventional SMILES crystals (Figure 2C–K), due to the much lower optical density and thus negligible reabsorption. Using this "lattice dilution" approach, non-quenched, monoexponential fluorescence lifetimes were resolved for all five fluorophores tested (Figures 2I–K and S5), confirming that energy migration is indeed responsible for the relatively short and non-mono-exponential lifetimes as well as reduced quantum yields seen in parent SMILES materials. Figure 2I–K compares the excitation and emission spectra of cyanine (DiOC2), rhodamine 3B (Rh3B), and oxazine in different environments. Remaining graphs representing diazaoxatriangu-

lenium (DAOTA) and styryl dye LDS751 are shown in Figure S5. Once SMILES crystals are ground to particles small enough to minimize the reabsorption effect (around 2  $\mu$ m), they show spectra almost identical to the dye in solution and diluted in TBA·CS<sub>2</sub>PF<sub>6</sub> crystals. For each dye, two different solvents were included in the comparison, in order to indicate the degree of solvatochromism displayed by each dye, which reflect their susceptibility to the local dielectric environment. The optical density of the TBA-diluted samples was too low to obtain reliable quantum yields. Yet, from the observed monoexponential fluorescence lifetimes and the radiative lifetimes measured for solution, we can estimate these values (Table S2). In the case of cyanine (Figure 2I), the estimated quantum yield ( $\Phi = 0.49$ ) in the TBA·CS<sub>2</sub>PF<sub>6</sub> crystal exceeds the quantum yield in DCM ( $\Phi = 0.06$ ), indicating restricted rotational freedom of this flexible fluorophore in the solid state, which was further confirmed by comparison to the dye diluted in a solid polystyrene thin film ( $\Phi = 0.44$ ). Also, Rh3B increases its quantum yield from 0.7 in solution to 0.9 in the TBA·CS<sub>2</sub>PF<sub>6</sub> crystal, hinting toward a decreased non-radiative decay rate in the solid state. Oxazine is a particularly interesting example. Its quantum yield in the neat SMILES crystal was quite low ( $\Phi = 0.02$ ) and only moderately increased relative to the dye-only crystal (Figures 1E and 2K). However, a dramatic improvement in its quantum yield ( $\Phi$  = 0.85), also exceeding that of solution ( $\Phi = 0.71$ ), can be seen once oxazine is diluted in the TBA·CS<sub>2</sub>PF<sub>6</sub> crystal. These observations highlight the fact that the non-ideal quantum yields of neat SMILES crystals are not due to interactions with the CS-anion complexes constituting the isolation lattice but rather a consequence of the relatively high exciton mobility (Table S1) and the presence of chemical impurities<sup>55</sup> or other

To demonstrate that observed properties are not limited to slowly grown single crystals and are reproducible in other solid-state materials, we also prepared all five dyes as microcrystalline powders of TBA-diluted SMILES by fast precipitation in heptane and as spin-cast thin films. Each of them showed very similar results (Figure S6). These experiments confirm that the remaining quenching in SMILES materials originates from exciton migration to trap states and, importantly, that the CS-anion complex lattice of SMILES allow perfect reproduction of spectral properties, fluorescence lifetimes, and quantum yields intrinsic to molecular dyes.

To reach the full potential of SMILES materials, either trap states have to be removed or exciton migration to traps have to be prohibited without dilution. Increasing the purity and quality of the crystal is always desirable. However, as the energy migration in dense molecular materials easily involves hundreds or even thousands of dye units, higher purity and crystal quality are unlikely to be a general solution, in particular when preparing nanoparticles or thin films with large surface areas or many domain boundaries (interfaces) and correspondingly more defects. To obtain the highest possible brightness per volume, a different approach is necessary: one that allows high quantum yields and control of excited-state lifetimes in materials with high-dye densities, efficient energy migration, and the ubiquitous presence of trap/defect sites.

Doping as a Universal Solution to the Brightness Problem in Solid-State Emitters. A key feature of SMILES crystals is the very similar packing of different cationic dyes, always alternatingly stacked with the CS—anion complexes, as sketched in Figure 1A.<sup>45,46</sup> This persistent packing motif

suggests that different dyes may mix together in SMILES. If possible, doping of a SMILES system with a more red-shifted dye acting as a FRET acceptor should allow fast and efficient energy transfer to the dopant dye (Figure 3A). With the optimal degree of doping, it should be possible to outcompete migration to traps and lock the exciton on the dopant. Consequently, the excited state will decay with fluorescence spectra, and lifetimes determined by the intrinsic properties of

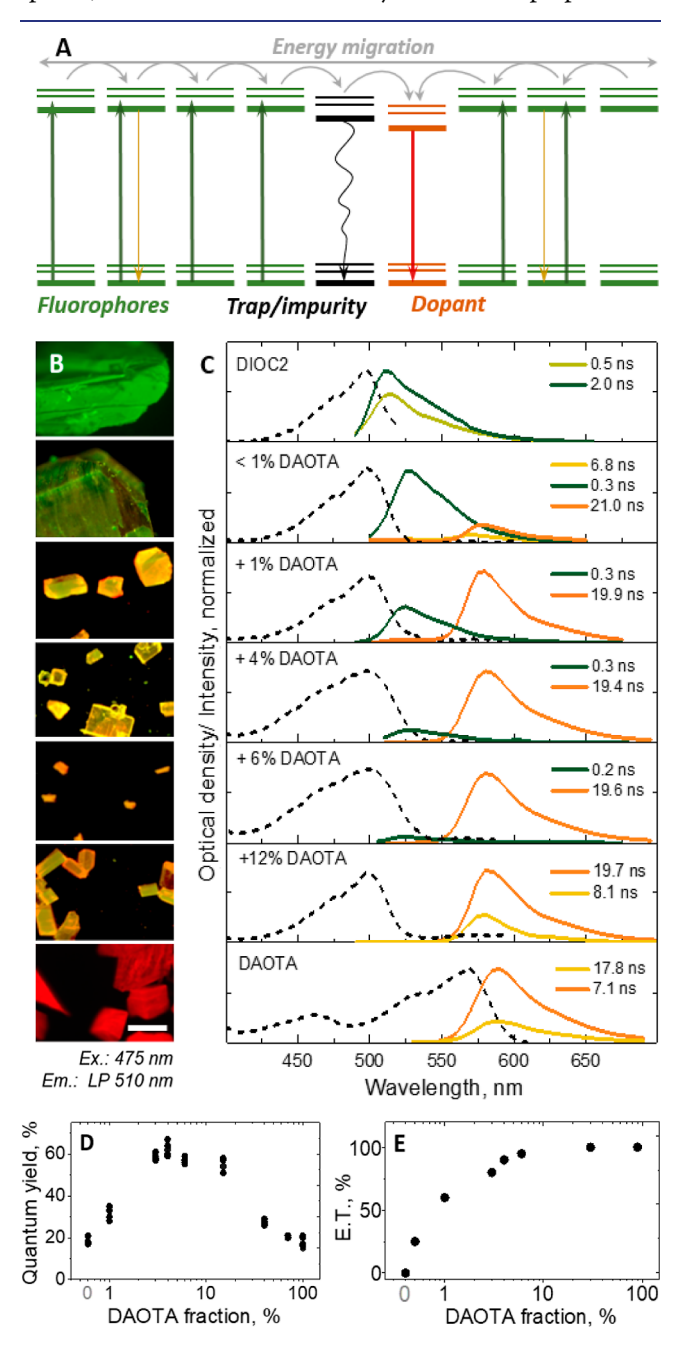


Figure 3. (A) State diagram representing FRET-based SMILES crystals. (B) Fluorescence micrographs (ex 475 nm, em. 510 nm LP, scale bar—100  $\mu m)$  of cyanine (DiOC2) and DAOTA-based SMILES crystals at varying DiOC2/DAOTA ratios. (C) Fluorescence excitation and decay-associated emission spectra as a function of DAOTA doping (ground crystals from panel B). (D) Changes in the quantum yield of as a function of DAOTA doping. (E) Energy-transfer efficiency in DiOC2-DAOTA FRET SMILES crystals as a function of DAOTA doping.

the dopant, as observed in the diluted  $TBA \cdot CS_2 PF_6$  system and in dilute solutions. The red-shifted emission of the dopant relative to the main absorber (donor dye), in this FRET SMILES system should at the same time solve the problem of reabsorption.

To explore this FRET-based doping strategy for improving and tailoring the performance of SMILES, we first grew SMILES crystals of the cyanine dye (DiOC2) in the presence of increasing amounts of the DAOTA fluorophore. Figure 3B shows fluorescence micrographs of DiOC2 SMILES crystals with increasing doping of DAOTA. The dominance of the yellow DAOTA emission is already clearly seen at 1% doping. A more quantitative measure is obtained from the excitation and emission spectra of the ground crystals (Figure 3C). Excitation spectra are practically invariant upon doping and resemble those of DiOC2, emphasizing that it is by far the dominating absorber, both due to its excess and almost 10-fold higher molar absorption coefficient (Table S1).

Decay-associated fluorescence spectra (Figure 3C) show, as expected, that emission from the neat (100%) DiOC2 SMILES crystals are non-mono-exponential and requires at least two decay components (0.5 and 2 ns) to be fitted. For the doped systems, the decay-associated emission spectra allow deconvolution of the donor and acceptor emission bands. Importantly, up to 6% doping, the DAOTA acceptor shows monoexponential decay with  $\approx 20$  ns fluorescence lifetime and an emission peak around 578 nm, in very good agreement with its solution properties<sup>56</sup> and when diluted in TBA·CS<sub>2</sub>PF<sub>6</sub> SMILES crystals (Figure S5A,B,E and Table S2). However, at 12% DAOTA doping, the DAOTA decay becomes nonmono-exponential, indicating that now excitons are not fully locked on isolated DAOTA sites but can migrate in-between DAOTA sites and thereby reach trap states. This interpretation is also reflected in the emission quantum yields that peak at doping levels of 4–6 mol % (Figure 3D) with  $\Phi$  = 0.58. The relative FRET efficiency, calculated as the ratio between the donor and acceptor emissions, clearly indicate efficient energy transfer to the DAOTA acceptor at relatively low concentrations, reaching >90% already at ~4% DAOTA loading (Figure 3E). We determined the actual doping degree by dissolving individual crystals and measuring their absorption spectra. This procedure revealed that the incorporation of the dopant varies from crystal to crystal.

To avoid inter-crystal variability and to obtain more reproducible embodiments of FRET SMILES materials, we also prepared micro-crystalline powders and spin-cast thin films by fast quantitative precipitation/evaporation of precursor (DCM) solutions (see Experimental Section, Supporting Information for more details). These samples display high homogeneity and reproducibility. Photophysical properties measured as a function of doping levels (Figures S7) are very similar to the larger crystals, though with more efficient FRET transfer, reaching 100% already at ~1 mol % DAOTA, and with slightly lower maximum quantum yields for spin-coated films ( $\Phi$  = 0.52). We interpret these differences as resulting from more homogeneous distribution of the dopant in the fast precipitated systems compared to slowly grown crystals. However, the quantum yield does not increase to the same degree as a result of the higher density of trap sites/ defects, in particular, in thin films. 12,45 For the microcrystalline powders, X-ray diffraction indicates that the packing in neat DiOC2 SMILES powders is similar to that reported for single crystals with alternating stacking of cations and anion

complexes (Figure S8). Furthermore, we found that this lattice is unaffected by introduction of DAOTA at the low doping levels ( $\leq$ 5 mol %) in the FRET SMILES powders (Figure S9) that display optimal optical properties.

The universality of FRET SMILES was explored by preparation of systems with Rh3B as the acceptor (dopant) for DiOC2 and with Rh3B as the donor lattice accommodating oxazine as the red-shifted dopant and emitter. Figures 4 and S10 show the properties of the micro-crystalline embodiments of these systems, while data for thin films and slowly grown larger crystals are given in Figures S11 and S12. Overall, these systems perform very similarly to the DAOTA-doped DiOC2 system for all three sample types, displaying highly improved

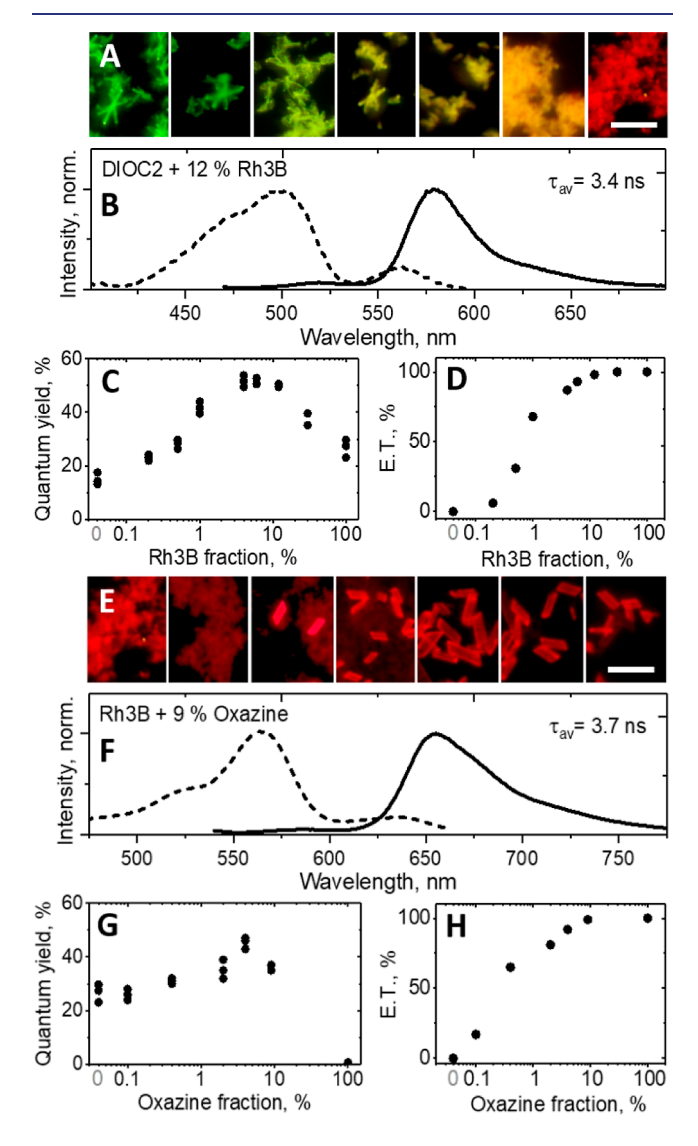


Figure 4. FRET SMILES micro-crystals. (A,E) Fluorescence micrographs (ex 475 nm, em. 510 nm LP, scale bar—3  $\mu$ m) of cyanine; DiOC2 (A) and Rh3B (E) SMILES micro-crystals at varying donor/acceptor ratios. (B,F) Fluorescence excitation and emission spectrum of indicated FRET SMILES micro-crystals. (C,G) Changes in the quantum yield of DiOC2-Rh3B (C) and Rh3B-oxazine (G) SMILES microcrystals as a function of increasing fraction of an acceptor (Rh3B or oxazine, respectively). (D,H) Changes in energy-transfer efficiency in DiOC2-Rh3B (D) and Rh3B-oxazine (H) SMILES micro-crystals as a function of increasing fraction of an acceptor (Rh3B or oxazine, respectively).

fluorescence quantum yields and lifetimes, confirming the robustness of the approach for various dyes and various dye combinations.

Programmable Lifetimes in FRET SMILES. The emission spectra of Rh3B and DAOTA are very similar  $(\lambda_{\rm fl} \approx 580 \text{ nm})$  as are the spectral properties of the two FRET SMILES materials with these two dyes as acceptors and DiOC2 as the donor (compare, for example, Figures 3C and 4B). However, their emission lifetimes are very different:  $\tau =$ 3.5 ns for DiOC2-Rh3B and  $\tau$  = 19 ns for DOIC2-DAOTA, exemplifying how FRET SMILES enable straightforward emission lifetime design of solid materials, directly from wellknown solution-state molecular properties.

FRET SMILES Outperform FRET Doping in Non-SMILES Materials. Doping of organic emissive materials with red-shifted dyes for tuning of the emission color has been reported for many polymer and small-molecule materials, including OLEDs and nanoparticles, and has in several cases also been reported to improve the overall emission yield. 50,57,58 However, in several cases, it is also noticed that not all dye combinations are successful. 49,59,60

To further elucidate the properties of SMILES and doped FRET SMILES materials, we turned to studying the doping of the corresponding non-SMILES materials. Microcrystalline powders of neat dyes doped with variable fractions of redshifted dyes were prepared in the same manner as the doped SMILES powders described above, and their emission properties were studied. The neat cyanine dye (DiOC2·PF<sub>6</sub>) powder show a red-shifted and dimmed emission compared to the fluorophore in solution and in SMILES materials (Figure S13). Doping with increasing amounts of Rh3B did not improve the brightness. On the contrary, emission quantum yields dropped further from 0.5% to <0.2% with increasing amount of Rh3B doping (bottom, Figure 5), compared to the corresponding FRET SMILES microcrystalline powders, which increase from 18 to 54% (top, Figure 5). Doping of DiOC2

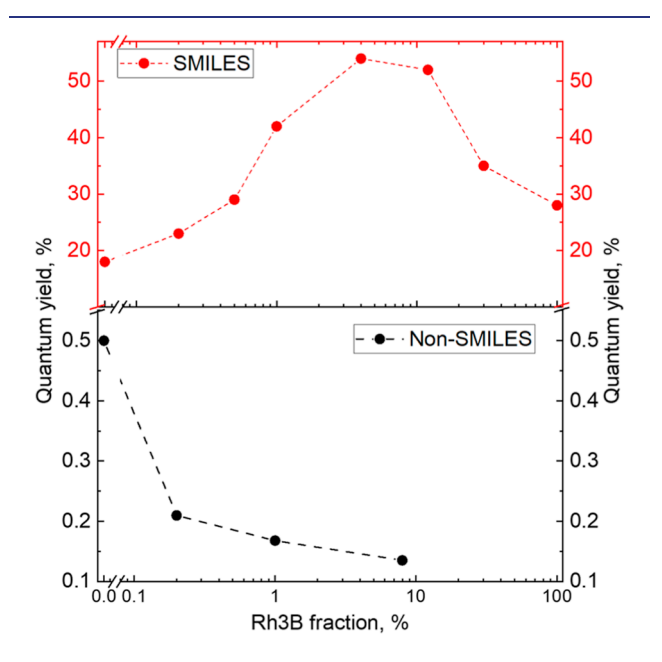


Figure 5. Quantum yield of neat (non-SMILES) DiOC2 microcrystalline powders doped with Rh3B (black points, lower panel). For comparison, the quantum yield of SMILES microcrystalline powders of DiOC2 doped with Rh3B (red points, upper panel) is also given.

with DAOTA and doping of Rh3B with oxazine also failed to improve the low quantum yields of the non-SMILES powders (Figure S14). Doping of DiOC2 with Rh3B or DAOTA clearly leads to emission from the dopants (Figures S15 and S16) and quenching of the cyanine, showing that energy transfer indeed does occur. In the case of Rh3B doped with oxazine, however, it seems that energy transfer is much less efficient. This outcome is likely due to the large red shift of the Rh3B emission in the aggregated state, which makes oxazine inefficient as the FRET acceptor. The very low emission yields (<0.3%) of non-SMILES DiOC2 doped with Rh3B and DAOTA suggest that the dopants are quenched by the cyanine matrix. A likely mechanism for this quenching is photoinduced electron transfer (PET). The relative HOMO energies for DiOC2, Rh3B, and DAOTA (Figure S17) support that reductive PET from DiOC2 to excited Rh3B and DAOTA dopants will be favorable. Such failure of doped emitter materials due to PET quenching has been reported for other materials.60

These results highlight that doping is not a general solution to solid-state self-quenching in non-SMILES materials. Furthermore, they show that the structural isolation of dyes between the CS-anion complexes in SMILES materials prohibits otherwise favorable PET quenching (as illustrated in Figure 6). This allows a broad range of donor dyes and

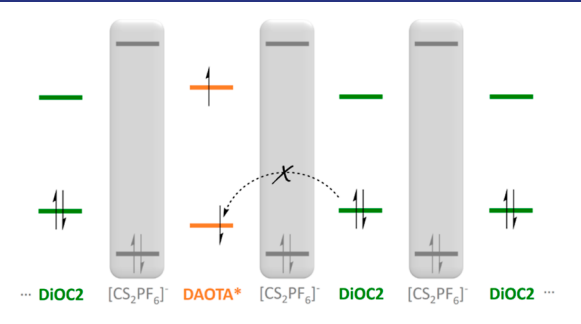


Figure 6. Schematic model with a molecular orbital diagram for doped SMILES with the acceptor DAOTA in its S1 state. Reductive PET from the DiOC2 donor does not take place across the CS-anion complex [CS2PF6], even though PET is energetically favorable according to the relative HOMO energies.

dopants to be combined in SMILES materials to tailor spectral and photophysical properties without severe limitations imposed by PET quenching. This makes dye doping a much more general solution when combined with the SMILES

Very Weak Electronic Coupling and Efficient FRET **Are Properties of SMILES.** The results from doping of both SMILES and non-SMILES materials emphasize important properties of SMILES. (1) In agreement with the model of electronic coupling shown in Figure 1D, strong electronic coupling is efficiently prohibited in SMILES. This is witnessed by the small spectral shifts that fully can be explained by variations in the dielectric environment (see, for example, Figure 2I–K), 12 as well as the insignificant changes in radiative lifetimes from the dilute solution to neat SMILES materials (Table S2). (2) SMILES support very weak coupling, though still efficient FRET-based energy transfer. Thus, excitations are localized on single dyes but will jump between dye sites by Förster-type energy transfer. With interdye spacing of 15-20 Å, comparable to the size of the chromophores, the point dipole approximation of the Förster equation is probably

Table 1. Maximum Brightness per Volume of Various SMILES-Based Solid-State Materials, Calculated Using an Average Lattice Volume of 3.5 nm<sup>3</sup>

|                 | maximum brightness per volume $(B_{\rm V})$ , ${\rm M}^{-1}~{\rm cm}^{-1}~{\rm nm}^{-3}$ |             |         |       |                     |                     |                     |
|-----------------|--|-------------|---------|-------|---------------------|---------------------|---------------------|
|                 |  | neat SMILES |         |       | FRET SMILES         |                     |                     |
|                 | hypothetical maximum $B_{\rm V}$ in solid state <sup>a</sup>                             | crystals    | powders | films | crystals            | powders             | films               |
| cyanine (DiOC2) | 95,000   | 11,800      | 8100    | 5300  |                     |                     |                     |
| DAOTA           | 20,000   | 1500        | 1900    | 1800  | 27,500 <sup>b</sup> | 30,300 <sup>b</sup> | 24,600 <sup>b</sup> |
| rhodamine 3B    | 105,000  | 9700        | 7800    | 5500  | 32,200 <sup>c</sup> | 25,500 <sup>c</sup> | 22,700°             |
| oxazine         | 90,000   | 600         | 600     | 700   | 19,400 <sup>d</sup> | 13,500 <sup>d</sup> | 12,400 <sup>d</sup> |

<sup>a</sup>Calculated from photophysical properties in dilute (solid) solution and assuming close packing of neat dye molecules. <sup>b</sup>DiOC2-DAOTA FRET SMILES system, with 6% DAOTA doping for crystals and 5% DAOTA doping for powders and films. DiOC2-Rh3B FRET SMILES system, with 8% Rh3B doping for crystals, 4% for powders, and 7% for films. dRh3B-oxazine FRET SMILES system, with 5% oxazine doping for crystals, 8% for powders, and 8% for films.

insufficient for quantitative predictions of FRET rates, yet they are still expected to scale with the spectral overlap intergrals.<sup>3</sup> We notice that relative high fractions of dopants 1-5% are required to achieve efficient FRET transfer to the dopants (Figures 3E, 4D,H, S7, and S10-S12). This need for higherdopant levels reflects a moderate transfer rate and exciton diffusion length within the SMILES donor lattice even compared to systems with isolation of dyes in other guest matrixes, where efficient transfer has been reported to occur at much lower doping levels. 34,50,60 This interpretation further emphasizes the structural and electronic isolation of dyes in SMILES that only allow very weak coupling and consequently exciton transfer that occurs by FRET.

**Super-bright FRET SMILES.** The significant improvement in optical properties of FRET SMILES with low acceptor concentrations over single-fluorophore SMILES can best be seen in terms of brightness per volume values  $(B_V)$  and quantum yields summarized in Tables 1 and S3. While the quantum yield of neat DAOTA SMILES crystals was previously reported to be ~25%, FRET SMILES crystals doped with DAOTA reach a quantum yield of ~60% (Figure 3D). The effect is even more dramatic for thin films, where neat SMILES films were found to give quantum yields of only a few percent<sup>45</sup> (Table S3), due to the higher defect density. With doping, however, quantum yields increase to  $\Phi = 52\%$ , making super-bright thin films readily available by the FRET SMILES approach. Taking into account the high packing density in the SMILES crystals (volume per dye being typically below 4 nm<sup>3</sup>, Table S3), the high molar absorption coefficients of the donor dyes (Table S2) and quantum yields now reaching 60-65%, the volume-normalized brightness of such FRET SMILES materials reaches as high as  $B_V = 32,200 \text{ M}^{-1}$ cm<sup>-1</sup> nm<sup>-3</sup>. The doping of SMILES materials improves the brightness even relative to the best single-dye SMILES (e.g., Rh3B) by a factor of 3, while weaker absorbers (e.g., DAOTA) and more quenched dyes (e.g., oxazine) are improved by more than 1 order of magnitude.

Impressively, the brightness of FRET SMILES materials is now approaching the hypothetical value expected for nonquenched and undiluted dye solids (Table 1). In the case of DiOC2-DAOTA FRET SMILES, the observed  $B_V$  even exceeds this hypothetical value as a result of the highly increased absorption inherited from the DiOC2 donor. This is even true for the defect-prone thin films. These brightness values clearly exceed those obtained by other general methods for bright-dye-based materials like AIEs, conjugated polymer nanoparticles, and dye-FRET pairs in polymer particles as well.41,61,62

## CONCLUSIONS

We have created a universal concept for super-bright, organic, solid-state emitters by doping SMILES with FRET acceptors. Reproduction of solution-like spectra, emission lifetimes, and quantum yields from cationic dyes embedded in the TBA. CS<sub>2</sub>PF<sub>6</sub> crystal shows that the CS-anion complexes forming SMILES have no negative impact on fluorophore photophysics and that the non-optimal photophysical properties result solely from macroscopic effects (self-absorption/inner filter effects) and mesoscopic effects (exciton migration to trap sites). Both of these effects can be eliminated using the FRET SMILES approach. Exploiting the intrinsically fast energy transfer between the fluorophores in SMILES materials, mobile excitons can be funneled to and locked on the introduced dopants, increasing the material brightness to unprecedentedly high values. The doping strategy significantly widens the scope of SMILES, making the materials robust to chemical and structural defects, as exemplified by the large improvements in the brightness and quantum yields of oxazine emitters and thin films in general. Furthermore, the suppression of PET quenching in SMILES allows independent selection of the absorber (donor) dye and emitter (acceptor), which in turn eliminates the self-absorption problem and allows very high tunability of spectral properties and emission lifetimes.

#### ASSOCIATED CONTENT

## Supporting Information

The Supporting Information is available free of charge at https://pubs.acs.org/doi/10.1021/jacs.2c08540.

Experimental section; preparation of samples; additional spectra and micrographs; and a summary and comparison of photophysical properties (PDF)

## AUTHOR INFORMATION

## **Corresponding Authors**

Amar H. Flood - Department of Chemistry, Indiana University, Bloomington 47405 Indiana, United States; orcid.org/0000-0002-2764-9155; Email: aflood@ indiana.edu

Bo W. Laursen - Nano-Science Center & Department of Chemistry, University of Copenhagen, Copenhagen 2100, Denmark; o orcid.org/0000-0002-1120-3191; Email: bwl@chem.ku.dk

#### **Authors**

Laura Kacenauskaite – Nano-Science Center & Department of Chemistry, University of Copenhagen, Copenhagen 2100, Denmark

Stine G. Stenspil – Nano-Science Center & Department of Chemistry, University of Copenhagen, Copenhagen 2100, Denmark; orcid.org/0000-0002-0252-6829

Andrew H. Olsson – Department of Chemistry, Indiana University, Bloomington 47405 Indiana, United States

Complete contact information is available at: https://pubs.acs.org/10.1021/jacs.2c08540

#### **Author Contributions**

The manuscript was written through contributions of all authors. All authors have given approval to the final version of the manuscript.

#### **Notes**

The authors declare no competing financial interest.

#### ACKNOWLEDGMENTS

This work was supported by the Danish Council of Independent Research (DFF-0136-00122B) and by the National Science Foundation (DMR-2118423). We acknowledge input from Maren Pink, Department of Chemistry, Indiana University on interpretation of powder X-ray data.

#### ABBREVIATIONS

AIE aggregation-induced emission

CS cyanostar (pentacyanopentabenzo[25]annulene)

DAOTA diazaoxatriangulenium DCM dichloromethane

DiOC2 3,3'-diethyloxacarbocyanine

ET energy transfer

FRET Förster resonance energy transfer

LDS751 2-[(1*E*,3*E*)-4-[4-(dimethylamino)phenyl]buta-1,3-

dienyl]-1-ethyl-N,N-dimethylquinolin-1-ium-6-

amine perchlorate

LP long-pass filter

MOF metal—organic framework
OLED organic light-emitting diode
PET photoinduced electron transfer

Q.Y. quantum yield Rh3B rhodamine 3B

SMILES small-molecule ionic isolation lattices

TBA tetrabutylammonium cations

## REFERENCES

- (1) Russ, B.; Glaudell, A.; Urban, J. J.; Chabinyc, M. L.; Segalman, R. A. Organic thermoelectric materials for energy harvesting and temperature control. *Nat. Rev. Mater.* **2016**, *1*, 16050.
- (2) Someya, T.; Bao, Z.; Malliaras, G. G. The rise of plastic bioelectronics. *Nature* **2016**, 540, 379–385.
- (3) van de Burgt, Y.; Melianas, A.; Keene, S. T.; Malliaras, G.; Salleo, A. Organic electronics for neuromorphic computing. *Nat. Electron.* **2018**, *1*, 386–397.
- (4) Sirringhaus, H. 25th Anniversary Article: Organic Field-Effect Transistors: The Path Beyond Amorphous Silicon. *Adv. Mater.* **2014**, 26. 1319–1335.
- (5) Wang, Z.; Yu, F.; Chen, W.; Wang, J.; Liu, J.; Yao, C.; Zhao, J.; Dong, H.; Hu, W.; Zhang, Q. Rational Control of Charge Transfer Excitons Toward High-Contrast Reversible Mechanoresponsive Luminescent Switching. *Angew. Chem., Int. Ed. Engl.* **2020**, *59*, 17580–17586.

- (6) Liu, D.; De, J.; Gao, H.; Ma, S.; Ou, Q.; Li, S.; Qin, Z.; Dong, H.; Liao, Q.; Xu, B.; Peng, Q.; Shuai, Z.; Tian, W.; Fu, H.; Zhang, X.; Zhen, Y.; Hu, W. Organic Laser Molecule with High Mobility, High Photoluminescence Quantum Yield, and Deep-Blue Lasing Characteristics. *J. Am. Chem. Soc.* **2020**, *142*, 6332–6339.
- (7) Stolte, M.; Schembri, T.; Süß, J.; Schmidt, D.; Krause, A.-M.; Vysotsky, M. O.; Würthner, F. 1-Mono- and 1,7-Disubstituted Perylene Bisimide Dyes with Voluminous Groups at Bay Positions: In Search for Highly Effective Solid-State Fluorescence Materials. *Chem. Mater.* 2020, 32, 6222–6236.
- (8) Dong, H.; Fu, X.; Liu, J.; Wang, Z.; Hu, W. 25th Anniversary Article: Key Points for High-Mobility Organic Field-Effect Transistors. *Adv. Mater.* **2013**, 25, 6158–6183.
- (9) Sisto, T. J.; Zhong, Y.; Zhang, B.; Trinh, M. T.; Miyata, K.; Zhong, X.; Zhu, X. Y.; Steigerwald, M. L.; Ng, F.; Nuckolls, C. Long, Atomically Precise Donor—Acceptor Cove-Edge Nanoribbons as Electron Acceptors. *J. Am. Chem. Soc.* **2017**, *139*, 5648—5651.
- (10) Jenekhe, S. A.; Osaheni, J. A. Excimers and Exciplexes of Conjugated Polymers. *Science* **1994**, *265*, 765–768.
- (11) Bialas, D.; Kirchner, E.; Röhr, M. I. S.; Würthner, F. Perspectives in Dye Chemistry: A Rational Approach toward Functional Materials by Understanding the Aggregate State. *J. Am. Chem. Soc.* **2021**, *143*, 4500–4518.
- (12) Gierschner, J.; Shi, J.; Milián-Medina, B.; Roca-Sanjuán, D.; Varghese, S.; Park, S. Luminescence in Crystalline Organic Materials: From Molecules to Molecular Solids. *Adv. Opt. Mater.* **2021**, *9*, 2002251.
- (13) Kasha, M.; Rawls, H. R.; El-Bayoumi, M. A. The exciton model in molecular spectroscopy. *Pure Appl. Chem.* **1965**, *11*, 371–392.
- (14) Cornil, J.; Beljonne, D.; Calbert, J.-P.; Brédas, J.-L. Interchain Interactions in Organic  $\pi$ -Conjugated Materials: Impact on Electronic Structure, Optical Response, and Charge Transport. *Adv. Mater.* **2001**, 13, 1053–1067.
- (15) Zhu, W.; Zheng, R.; Zhen, Y.; Yu, Z.; Dong, H.; Fu, H.; Shi, Q.; Hu, W. Rational Design of Charge-Transfer Interactions in Halogen-Bonded Co-crystals toward Versatile Solid-State Optoelectronics. *J. Am. Chem. Soc.* **2015**, *137*, 11038–11046.
- (16) Fratini, S.; Nikolka, M.; Salleo, A.; Schweicher, G.; Sirringhaus, H. Charge transport in high-mobility conjugated polymers and molecular semiconductors. *Nat. Mater.* **2020**, *19*, 491–502.
- (17) Lin, Y.; Wang, J.; Zhang, Z.-G.; Bai, H.; Li, Y.; Zhu, D.; Zhan, X. An Electron Acceptor Challenging Fullerenes for Efficient Polymer Solar Cells. *Adv. Mater.* **2015**, *27*, 1170–1174.
- (18) Currie, M. J.; Mapel, J. K.; Heidel, T. D.; Goffri, S.; Baldo, M. A. High-Efficiency Organic Solar Concentrators for Photovoltaics. *Science* **2008**, 321, 226–228.
- (19) Yoon, J.; Li, L.; Semichaevsky, A. V.; Ryu, J. H.; Johnson, H. T.; Nuzzo, R. G.; Rogers, J. A. Flexible concentrator photovoltaics based on microscale silicon solar cells embedded in luminescent waveguides. *Nat. Commun.* **2011**, *2*, 343.
- (20) Sandanayaka, A. S. D.; Matsushima, T.; Bencheikh, F.; Yoshida, K.; Inoue, M.; Fujihara, T.; Goushi, K.; Ribierre, J.-C.; Adachi, C. Toward continuous-wave operation of organic semiconductor lasers. *Sci. Adv.* 2017, 3, No. e1602570.
- (21) Hou, X.; Ke, C.; Bruns, C. J.; McGonigal, P. R.; Pettman, R. B.; Stoddart, J. F. Tunable solid-state fluorescent materials for supramolecular encryption. *Nat.Commun.* **2015**, *6*, 6884.
- (22) Wu, C.; Bull, B.; Szymanski, C.; Christensen, K.; McNeill, J. Multicolor Conjugated Polymer Dots for Biological Fluorescence Imaging. ACS Nano 2008, 2, 2415–2423.
- (23) Cheung, S.; O'Shea, D. F. Directed self-assembly of fluorescence responsive nanoparticles and their use for real-time surface and cellular imaging. *Nat.Commun.* **2017**, *8*, 1885.
- (24) Reisch, A.; Klymchenko, A. S. Fluorescent Polymer Nanoparticles Based on Dyes: Seeking Brighter Tools for Bioimaging. *Small* **2016**, *12*, 1968–1992.
- (25) Yang, J.-S.; Swager, T. M. Porous Shape Persistent Fluorescent Polymer Films: An Approach to TNT Sensory Materials. *J. Am. Chem. Soc.* **1998**, *120*, 5321–5322.

- (26) Schmidt, D.; Stolte, M.; Süß, J.; Liess, A.; Stepanenko, V.; Würthner, F. Protein-like Enwrapped Perylene Bisimide Chromophore as a Bright Microcrystalline Emitter Material. *Angew. Chem., Int. Ed.* **2019**, *58*, 13385–13389.
- (27) Pan, C.; Sugiyasu, K.; Wakayama, Y.; Sato, A.; Takeuchi, M. Thermoplastic fluorescent conjugated polymers: benefits of preventing  $\pi$ - $\pi$  stacking. *Angew. Chem., Int. Ed. Engl.* **2013**, 52, 10775–10779.
- (28) Würthner, F. Aggregation-Induced Emission (AIE): A Historical Perspective. *Angew. Chem., Int. Ed.* **2020**, *59*, 14192–14196.
- (29) Zhao, Z.; Zhang, H.; Lam, J. W. Y.; Tang, B. Z. Aggregation-Induced Emission: New Vistas at the Aggregate Level. *Angew. Chem., Int. Ed.* **2020**, *59*, 9888–9907.
- (30) Jiang, H.-L.; Tatsu, Y.; Lu, Z.-H.; Xu, Q. Non-, Micro-, and Mesoporous Metal—Organic Framework Isomers: Reversible Transformation, Fluorescence Sensing, and Large Molecule Separation. *J. Am. Chem. Soc.* **2010**, *132*, 5586—5587.
- (31) Kundu, P. K.; Olsen, G. L.; Kiss, V.; Klajn, R. Nanoporous frameworks exhibiting multiple stimuli responsiveness. *Nat. Commun.* **2014**, *5*, 3588.
- (32) Calzaferri, G.; Huber, S.; Maas, H.; Minkowski, C. Host-Guest Antenna Materials. *Angew. Chem., Int. Ed.* **2003**, 42, 3732–3758.
- (33) Nguyen, T.-Q.; Wu, J.; Doan, V.; Schwartz, B. J.; Tolbert, S. H. Control of Energy Transfer in Oriented Conjugated Polymer-Mesoporous Silica Composites. *Science* **2000**, 288, 652–656.
- (34) Poulsen, L.; Jazdzyk, M.; Communal, J.-E.; Sancho-García, J. C.; Mura, A.; Bongiovanni, G.; Beljonne, D.; Cornil, J.; Hanack, M.; Egelhaaf, H.-J.; Gierschner, J. Three-Dimensional Energy Transport in Highly Luminescent Host—Guest Crystals: A Quantitative Experimental and Theoretical Study. *J. Am. Chem. Soc.* **2007**, *129*, 8585—8593
- (35) Kahr, B.; Gurney, R. W. Dyeing Crystals. Chem. Rev. 2001, 101, 893–952.
- (36) Ou, Z.-m.; Yao, H.; Kimura, K. Preparation and optical properties of organic nanoparticles of porphyrin without self-aggregation. *J. Photochem. Photobiol., A* **2007**, *189*, 7–14.
- (37) Bwambok, D. K.; El-Zahab, B.; Challa, S. K.; Li, M.; Chandler, L.; Baker, G. A.; Warner, I. M. Near-Infrared Fluorescent Nano-GUMBOS for Biomedical Imaging. *ACS Nano* **2009**, *3*, 3854–3860.
- (38) Yang, Y.; Sun, C.; Wang, S.; Yan, K.; Zhao, M.; Wu, B.; Zhang, F. Counterion-Paired Bright Heptamethine Fluorophores with NIR-II Excitation and Emission Enable Multiplexed Biomedical Imaging. *Angew. Chem., Int. Ed. Engl.* **2022**, *61*, No. e202117436.
- (39) Reisch, A.; Didier, P.; Richert, L.; Oncul, S.; Arntz, Y.; Mély, Y.; Klymchenko, A. S. Collective fluorescence switching of counterion-assembled dyes in polymer nanoparticles. *Nat. Commun.* **2014**, *5*, 4089.
- (40) Reisch, A.; Trofymchuk, K.; Runser, A.; Fleith, G.; Rawiso, M.; Klymchenko, A. S. Tailoring Fluorescence Brightness and Switching of Nanoparticles through Dye Organization in the Polymer Matrix. *ACS Appl. Mater. Interfaces* **2017**, *9*, 43030–43042.
- (41) Egloff, S.; Melnychuk, N.; Reisch, A.; Martin, S.; Klymchenko, A. S. Enzyme-free amplified detection of cellular microRNA by light-harvesting fluorescent nanoparticle probes. *Biosens. Bioelectron.* **2021**, 179, 113084.
- (42) Haketa, Y.; Sasaki, S.; Ohta, N.; Masunaga, H.; Ogawa, H.; Mizuno, N.; Araoka, F.; Takezoe, H.; Maeda, H. Oriented Salts: Dimension-Controlled Charge-by-Charge Assemblies from Planar Receptor—Anion Complexes. *Angew. Chem., Int. Ed.* **2010**, 49, 10079—10083.
- (43) Haketa, Y.; Urakawa, K.; Maeda, H. First decade of  $\pi$ -electronic ion-pairing assemblies. *Mol. Syst. Des. Eng.* **2020**, *5*, 757–771.
- (44) Lee, S.; Chen, C.-H.; Flood, A. H. A pentagonal cyanostar macrocycle with cyanostilbene CH donors binds anions and forms dialkylphosphate [3]rotaxanes. *Nat. Chem.* **2013**, *5*, 704–710.
- (45) Benson, C. R.; Kacenauskaite, L.; VanDenburgh, K. L.; Zhao, W.; Qiao, B.; Sadhukhan, T.; Pink, M.; Chen, J.; Borgi, S.; Chen, C.-H.; Davis, B. J.; Simon, Y. C.; Raghavachari, K.; Laursen, B. W.; Flood, A. H. Plug-and-Play Optical Materials from Fluorescent Dyes and Macrocycles. *Chem* **2020**, *6*, 1978–1997.

- (46) Qiao, B.; Hirsch, B. E.; Lee, S.; Pink, M.; Chen, C.-H.; Laursen, B. W.; Flood, A. H. Ion-Pair Oligomerization of Chromogenic Triangulenium Cations with Cyanostar-Modified Anions That Controls Emission in Hierarchical Materials. *J. Am. Chem. Soc.* 2017, 139, 6226–6233.
- (47) Chen, J.; Fateminia, S. M. A.; Kacenauskaite, L.; Bærentsen, N.; Grønfeldt Stenspil, S.; Bredehoeft, J.; Martinez, K. L.; Flood, A. H.; Laursen, B. W. Ultrabright Fluorescent Organic Nanoparticles Based on Small-Molecule Ionic Isolation Lattices. *Angew. Chem., Int. Ed. Engl.* **2021**, *60*, 9450–9458.
- (48) Chen, J. S.; Stenspil, S. G.; Kaziannis, S.; Kacenauskaite, L.; Lenngren, N.; Kloz, M.; Flood, A. H.; Laursen, B. W. Quantitative Energy Transfer in Organic Nanoparticles Based on Small-Molecule Ionic Isolation Lattices for UV Light Harvesting. *ACS Appl. Nano Mater.* **2022**, DOI: 10.1021/acsanm.2c01899.
- (49) Wu, C.; Zheng, Y.; Szymanski, C.; McNeill, J. Energy Transfer in a Nanoscale Multichromophoric System: Fluorescent Dye-Doped Conjugated Polymer Nanoparticles. *J. Phys. Chem. C* **2008**, *112*, 1772–1781.
- (50) Trofymchuk, K.; Reisch, A.; Didier, P.; Fras, F.; Gilliot, P.; Mely, Y.; Klymchenko, A. S. Giant light-harvesting nanoantenna for single-molecule detection in ambient light. *Nat. Photonics* **2017**, *11*, 657–663.
- (51) Kühn, H.; Petermann, K.; Huber, G. Correction of reabsorption artifacts in fluorescence spectra by the pinhole method. *Opt. Lett.* **2010**, 35, 1524–1526.
- (52) Kumar Panigrahi, S.; Kumar Mishra, A. Inner filter effect in fluorescence spectroscopy: As a problem and as a solution. *J. Photochem. Photobiol.*, C **2019**, 41, 100318.
- (53) Powell, R. C.; Soos, Z. G. Singlet exciton energy transfer in organic solids. *J. Lumin.* 1975, 11, 1–45.
- (54) Newsome, W. J.; Ayad, S.; Cordova, J.; Reinheimer, E. W.; Campiglia, A. D.; Harper, J. K.; Hanson, K.; Uribe-Romo, F. J. Solid State Multicolor Emission in Substitutional Solid Solutions of Metal—Organic Frameworks. *J. Am. Chem. Soc.* **2019**, *141*, 11298—11303.
- (55) We do not propose any specific impurities, since this is a general observation and not related to a specific compound, but commercial dyes are usually listed as >95% pure. Impurities may include byproducts from synthesis or degradation products.
- (56) Bogh, S. A.; Simmermacher, M.; Westberg, M.; Bregnhøj, M.; Rosenberg, M.; De Vico, L.; Veiga, M.; Laursen, B. W.; Ogilby, P. R.; Sauer, S. P. A.; Sørensen, T. J. Azadioxatriangulenium and Diazaoxatriangulenium: Quantum Yields and Fundamental Photophysical Properties. *ACS Omega* **2017**, *2*, 193–203.
- (57) Gong, X.; Ma, W.; Ostrowski, J. C.; Bazan, G. C.; Moses, D.; Heeger, A. J. White Electrophosphorescence from Semiconducting Polymer Blends. *Adv. Mater.* **2004**, *16*, 615–619.
- (58) Chen, L.; Roman, L. S.; Johansson, D. M.; Svensson, M.; Andersson, M. R.; Janssen, R. A. J.; Inganäs, O. Excitation Transfer in Polymer Photodiodes for Enhanced Quantum Efficiency. *Adv. Mater.* **2000**, *12*, 1110–1114.
- (59) Peng, A.-D.; Xiao, D.-B.; Ma, Y.; Yang, W.-S.; Yao, J.-N. Tunable Emission from Doped 1,3,5-Triphenyl-2-pyrazoline Organic Nanoparticles. *Adv. Mater.* **2005**, *17*, 2070–2073.
- (60) Egelhaaf, H.-J.; Gierschner, J.; Oelkrug, D. Polarizability effects and energy transfer in quinquethiophene doped bithiophene and OPV films. *Synth. Met.* **2002**, *127*, 221–227.
- (61) Li, K.; Qin, W.; Ding, D.; Tomczak, N.; Geng, J.; Liu, R.; Liu, J.; Zhang, X.; Liu, H.; Liu, B.; Tang, B. Z. Photostable fluorescent organic dots with aggregation-induced emission (AIE dots) for noninvasive long-term cell tracing. *Sci. Rep.* **2013**, *3*, 1150.
- (62) Wu, C.; Schneider, T.; Zeigler, M.; Yu, J.; Schiro, P. G.; Burnham, D. R.; McNeill, J. D.; Chiu, D. T. Bioconjugation of Ultrabright Semiconducting Polymer Dots for Specific Cellular Targeting. J. Am. Chem. Soc. 2010, 132, 15410–15417.